Authors' Camera Ready Manuscript. To appear in the Proceedings of the 2017 IEEE 3rd International Conference on Electro-Technology for National Development (IEEE NIGERCON), Owerri, Nigeria, Nov 2017,
Please cite using bibliographic data of the associated published version.

H-infinity-PID Controller for an Open-loop Unstable System

Daniel N. Abara
Department of Electrical/Electronic Engineering
Cross River University of Technology, Calabar, Nigeria.
daniel.abara@crutech.edu.ng

Alexander Lanzon
School of Electrical & Electronic Engineering
The University of Manchester, England.
alexander.lanzon@manchester.ac.uk

***Abstract*— This paper proposes a H-infinity-PID cascade control technique for the control of an open-loop unstable system, the ball and beam system. This property of being open-loop unstable makes this system ideal for investigating the performance of different control techniques. A 5th order nonlinear model of the ball and beam plant is derived to include the actuation mechanism. A H-infinity-PID controller is proposed and applied to the system using a cascade structure. The control goal is to drive the ball to any desired position on the beam. A check for robustness of the closed loop is also performed using frequency domain methods. The results show that the proposed controller robustly stabilizes the system and equally achieves the setpoint tracking goal. The control voltage which is the control input is also found to be within practicable limits.**

***Index Terms*--PID, cascade, H-infinity, ball and beam, H-infinity-PID control, robust control, loop-shaping.**

I. INTRODUCTION

The ball and beam system (BBS) is an underactuated mechanical system, with two degrees of freedom. The system setup is made up of a beam which pivots in the vertical plane due to a Torque applied at the pivot, and a ball which is free to roll up and down the beam [1]. It has a very important property; it is open-loop unstable. That is, if there is no feedback control, the ball will roll off the beam when there is a small change in the beam angle. Aircraft, helicopters, underwater vehicles, mobile robots, and walking robots are real-life examples of systems that exhibit similar behaviour. Thus, research into such systems has a wide range of applications and control engineers have continued to study various control strategies such as PID, LQR, State feedback, etc. for the BBS. As reported in [2], out of over 11000 controllers in industry, most make use of PID feedback. This is probably due to its simplicity and the distinct effects of each of the three PID terms. However, PID controllers are typically not designed to be sensitive to system parameter variations although they possess some internal robustness. Hence, some authors have combined PID and other control techniques as in [3], which showed that fuzzy-PID yielded better performance than a PD controller only. Again, an optimal PID-PI cascade controller was proposed in [4] where a PID controller is related to a state feedback controller with integral action, and this 'optimal' PID controller is applied to the outer loop, while the inner loop is controlled using a PI controller, yielding better performance. In the references mentioned, and others on PID control of the BBS found in literature, it can be observed that there has been very few studies into the application of H-infinity synthesis to the BBS. Also, the research into the BBS has made use of mostly 2nd order and 4th order models which hardly take the actuation mechanism into account. In this paper, a 5th order model is derived which accounts for the actuator thereby enhancing practicability. Next, a robust controller is synthesized using the loop-shaping design method based on H-infinity synthesis [5] and applied in a cascade control scheme for the BBS.

II. SYSTEM MODELLING

The BBS setup considered and modelled in this study is the one composed of a beam which pivots in the vertical plane due to a Torque τ at the center/point of rotation; and a ball which rolls up and down the beam [1]. The nonlinear equations of motion of the rolling ball on beam, as derived in [6] and [7], using Lagrangian techniques, are given as:

$$\left(\frac{J_B}{R^2} + m\right)\ddot{r} - mr\dot{\theta}^2 + mg\sin\theta = 0. \qquad (1)$$

$$(J + mr^2)\ddot{\theta} + 2mr\dot{r}\dot{\theta} + mgr\cos\theta = \tau. \qquad (2)$$

The parameter descriptions and values are as follows: Mass of ball m = 0.111Kg, Radius of Ball, R = 0.015m, Beam moment of Inertia, J = 0.0172Kg.m^2, Ball moment of Inertia, J_B = 9.99×10^{-6}Kg.m^2, and Length of Beam, l = 1m. Equations (1) and (2) together form the nonlinear model of the Ball and beam system with the Torque τ as input and the ball position r as the output. This model does not include an actuator; hence a DC Motor is modelled next as the actuator of the system. Consider the armature circuit modelled in Fig 1. Applying, Kirchoff's voltage law [8]; we have that,

$$L\frac{di_A}{dt} + i_A R_A + K_B K_G\dot{\theta} = V_{IN}, \quad \{V_B = K_B K_G\dot{\theta}\} \qquad (3)$$

The parameter descriptions and values are: Armature Resistance, R_A = 11.9 Ohms, Armature Inductance, L_A = 0.3H, Voltage and Torque Constants, $K_T = K_B$ = 0.0148V.rad^{-1}s^{-1}, Gear ratio, K_G = 70, with $\dot{\theta}$ as the shaft velocity [9].

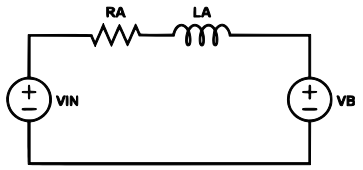

Figure 1. DC motor with input voltage V_{IN} (volts), resistance R_A (Ohms), inductance L_A (Henry), current i_A (Amperes) and the back-electromotive force V_B (volts).

The Torque generated is proportional to the armature current and is given by,

$$\tau = K_G K_T i_A. \quad (4)$$

Substituting (4) into (2), equation (2) becomes,

$$(J + mr^2)\ddot{\theta} + 2mr\dot{r}\dot{\theta} + mgr\cos\theta = K_G K_T i_A. \quad (5)$$

Equations (1), (3) and (5) together form the full nonlinear model for the BBS with the input as a Voltage V_{IN} and the output as the ball position r. Defining the state variables of the systems as, $x = [x_1\ x_2\ x_3\ x_4\ x_5]^T = [r\ \ \dot{r}\ \ \theta\ \ \dot{\theta}\ \ i_A]^T$, the nonlinear BBS can be represented as,

$$\begin{bmatrix}\dot{x_1}\\ \dot{x_2}\\ \dot{x_3}\\ \dot{x_4}\\ \dot{x_5}\end{bmatrix} = \begin{bmatrix} x_2 \\ B_1 x_1 x_4^2 - B_1 g \sin x_3 \\ x_4 \\ \frac{K_G K_T x_5 - 2mx_1x_2x_4 - mgx_1\cos x_3}{J+mx_1^2} \\ \frac{-R_A x_5 - K_B K_G x_4}{L_A}\end{bmatrix} + \begin{bmatrix}0\\0\\0\\0\\ \frac{1}{L_A}\end{bmatrix} V_{IN} \quad (6)$$

where $B_1 = \frac{m}{\frac{J_B}{R^2}+m}$.

III. PRELIMINARIES

The proposed control strategy involves two linear control schemes. The nonlinear model in (6) was therefore linearized using the Jacobian method presented in [10]. The Jacobian matrix of (6) with respect to the state variable x that is, $\frac{\partial f(x,V_{IN})}{\partial x}$ is given by,

$$\begin{bmatrix} 0 & 1 & 0 & 0 & 0 \\ B_1x_4^2 & 0 & -B_1 g\cos x_3 & 2B_1x_1x_4 & 0 \\ 0 & 0 & 0 & 1 & 0 \\ \frac{\partial f_4}{\partial x_1} & \frac{-2mx_1x_4}{J+mx_1^2} & \frac{mgx_1\sin x_3}{J+mx_1^2} & \frac{-2mx_1x_2}{J+mx_1^2} & \frac{K_TK_G}{J+mx_1^2} \\ 0 & 0 & 0 & \frac{-K_BK_G}{L_A} & \frac{-R_A}{L_A}\end{bmatrix} \quad (7)$$

where, $\frac{\partial f_4}{\partial x_1}$ is given as,

$$\frac{(J+mx_1^2)(-2mx_2x_4 - mg\cos x_3) - ((K_GK_Tx_5 - 2mx_1x_2x_4 - mgx_1\cos x_3)(2mx_1))}{(J+mx_1^2)^2}$$

Also, the Jacobian of (6) with respect to the control input V_{IN} is given in (8).

$$\frac{\partial f(x,V_{IN})}{\partial V_{IN}} = \begin{bmatrix}0\\0\\0\\0\\ \frac{1}{L_A}\end{bmatrix} \quad (8)$$

The ball operating point was selected as $r_0 = x_{1_0} = 0.25$m, and the operating point for the beam angle was chosen as $\theta_0 = x_{3_0} = 0$ rad, the ball velocity $\dot{r_0} = x_{2_0} = 0$, and the beam velocity $\dot{\theta_0} = x_{4_0} = 0$rad. Substituting these operating points into (2), the Torque required to hold this equilibrium is 0.27N. Substituting this Torque value into (4), the operating current i_A, is 0.26A. Hence, substituting all these parameters into (7) and (8), the linearized BBS in state space is given by (9) and (10 below;

$$\begin{bmatrix}\dot{x_1}\\ \dot{x_2}\\ \dot{x_3}\\ \dot{x_4}\\ \dot{x_5}\end{bmatrix} = \begin{bmatrix} 0 & 1 & 0 & 0 & 0 \\ 0 & 0 & -7 & 0 & 0 \\ 0 & 0 & 0 & 1 & 0 \\ -44.82 & 0 & 0 & 0 & 42.92 \\ 0 & 0 & 0 & -3.45 & -39.67\end{bmatrix}\begin{bmatrix}x_1\\x_2\\x_3\\x_4\\x_5\end{bmatrix} + \begin{bmatrix}0\\0\\0\\0\\3.33\end{bmatrix} V_{IN} \quad (9)$$

And since the ball position $r = x_1$ is the output, the C matrix is given as,

$$y = [1\ 0\ 0\ 0\ 0] \quad (10)$$

An open-loop analysis [11] was performed on the system to ascertain its conditions without control. The poles which are the eigenvalues of the A matrix in (10) are, λ_p = -35.4894, -5.9104, 3.5548, (-0.9108+3.9825j), (-0.9108-3.9825j) where p = 1,…,5 respectively. It is clear that the system is unstable without control since there is a pole in the right-half plane (λ_3 = 3.5548). The design of the control is given next.

IV. CONTROL DESIGN

The block diagram which depicts the control is given in Fig.2. below:

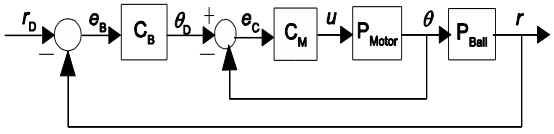

Figure 2. Cascade Control Scheme for H-infinity-PID controller.

In Fig. 2, C_B is the robust stabilizing controller from H-infinity synthesis, C_M is the PID controller, θ_D and θ are the desired and actual motor angle respectively, r_D and r are the desired and actual ball positions respectively, e_M and e_B are the errors in the motor angle and ball position respectively, and u is the control voltage.

A. PID Controller Design: Inner (DC motor) loop

A PID controller as described in [11] takes the form of (11) where $k_\mathrm{P}, k_\mathrm{I}, k_\mathrm{D}$ are the proportional, integral and derivative gains respectively, and e is the error between the set point and the measured output.

$$u(t) = k_\mathrm{P}e(t) + k_\mathrm{I}\int_0^t e(t)dt + k_\mathrm{D}\frac{d(e(t))}{dt} \tag{11}$$

Denoting the previously chosen operating points as $[x_{1_0}, x_{2_0}, x_{3_0}, x_{4_0}, x_{5_0}] = [r_0, 0, 0, 0, i_{\mathrm{A}_0}]$ and substituting symbolically into (7), without using real values, the following A matrix is obtained *in terms of the linearized parameters*,

$$\begin{bmatrix} 0 & 1 & 0 & 0 & 0 \\ 0 & 0 & -B_1 g & 0 & 0 \\ 0 & 0 & 0 & 1 & 0 \\ \frac{-m.g.J+m^2.g.r_0^2-2m.r_0.K_\mathrm{G}.K_\mathrm{T}.i_{\mathrm{A}_0}}{(J+m.r_0^2)^2} & \mathbf{0} & \mathbf{0} & \mathbf{0} & \frac{K_\mathrm{T}K_\mathrm{G}}{J+m.r_0^2} \\ 0 & 0 & 0 & \frac{-K_\mathrm{B}K_\mathrm{G}}{L_\mathrm{A}} & \frac{-R_\mathrm{A}}{L_\mathrm{A}} \end{bmatrix} \tag{12}$$

From the 4th row of (12), neglecting the term which is the coefficient of the r state, and taking it as a parametric uncertainty, the relation between the acceleration and the current is,

$$\ddot{\theta} = \left(\frac{K_\mathrm{T}K_\mathrm{G}}{J+m\delta_1^2}\right) i \tag{13}$$

Taking Laplace transform and rearranging, the transfer function from the current to the motor angle is,

$$\frac{\theta(s)}{I(s)} = \frac{\frac{K_\mathrm{T}K_\mathrm{G}}{J+m\delta_1^2}}{s^2} \tag{14}$$

Similarly, from the 5th row of (9) and (12), neglecting the term which is the coefficient of the $\dot{\theta}$ state as an uncertainty, the relation between the input voltage and current is,

$$\frac{di}{dt} = -\left(\frac{R_\mathrm{A}}{L_\mathrm{A}}\right) i + \frac{1}{L_\mathrm{A}} V_\mathrm{IN} \tag{15}$$

Taking Laplace transform of (15), the transfer function from the voltage to current is,

$$\frac{I(s)}{V_\mathrm{IN}(s)} = \frac{\frac{1}{L_\mathrm{A}}}{s+\frac{R_\mathrm{A}}{L_\mathrm{A}}} \tag{16}$$

Combining (14) and (16), the transfer function for the DC motor is,

$$P_\mathrm{Motor} = \frac{\theta(s)}{V_\mathrm{IN}(s)} = \frac{\frac{K_\mathrm{T}K_\mathrm{G}}{L_\mathrm{A}(J+m\delta_1^2)}}{s^3+\left(\frac{R_\mathrm{A}}{L_\mathrm{A}}\right)s^2} = \frac{143.1}{s^3+39.67s^2} \tag{17}$$

The PID controller was designed using pole placement to meet a settling time of 0.3s and an overshoot of 5% for the servomotor. The standard 2nd order equation is given as,

$$\frac{Y(s)}{Ref(s)} = \frac{{\omega_\mathrm{n}}^2}{s^2+2\zeta\omega_\mathrm{n}s+{\omega_\mathrm{n}}^2} \tag{18}$$

where ζ and ω_n are the damping ratio and natural frequency respectively. Using equations and relations from [11], the damping ratio ζ and natural frequency ω_n which correspond to 5% overshoot and 0.3s settling time were computed and obtained as, $\zeta = 0.707$ and $\omega_\mathrm{n} = 18.86\mathrm{rads}^{-1}$ respectively. Substituting these values in (18), the required characteristics equation was obtained as,

$$\frac{Output}{Input} = \frac{355.66}{s^2+26.67s+355.66} \tag{19}$$

The poles of (19) are -13.34 ± 13.34j which correspond to a time constant of 0.075s and a settling time of roughly 0.3s. The PID controller was then chosen as,

$$V_\mathrm{IN}(s) = k_\mathrm{P}\big(\theta_\mathrm{D}(s) - \theta(s)\big) + \frac{k_\mathrm{I}}{s}\big(\theta_\mathrm{D}(s) - \theta(s)\big) - k_\mathrm{D}s\theta(s) \tag{20}$$

Substituting (20) in (17), the closed loop transfer function is,

$$\frac{\theta(s)}{\theta_\mathrm{D}(s)} = \frac{143.1k_\mathrm{P}s+143.1k_\mathrm{I}}{s^4+39.67s^3+143.1k_\mathrm{D}s^2+143.1k_\mathrm{P}s+143.1k_\mathrm{I}} \tag{21}$$

Since (21) is 4th order, two poles at s = -16 and s = -23 were added to the desired characteristic equation in (19) to yield,

$$\frac{\theta(s)}{\theta_\mathrm{D}(s)} = \frac{355.66}{s^4+70s^3+1760^2+23700s+130980} \tag{22}$$

Hence, equating the coefficients of the denominator of the desired in (22) to those of the denominator of the closed loop transfer function in (21), the PID gains are obtained as, $k_\mathrm{P} = 165.62$, $k_\mathrm{I} = 915.30$, and $k_\mathrm{D} = 12.30$.

B. H-infinity loop Shaping Controller Design: Outer loop

The H-infinity loop-shaping controller was designed in three steps. The first is loop-shaping where weights are used to shape the plant to meet desired specifications. Next is to synthesize a H-infinity controller which robustly stabilizes the coprime factors of the shaped plant as described in [12]. The final step is the combination of the H-infinity controller and the loop-shaping weights resulting in a robust stabilizing controller which is implemented as depicted in Fig. 3.

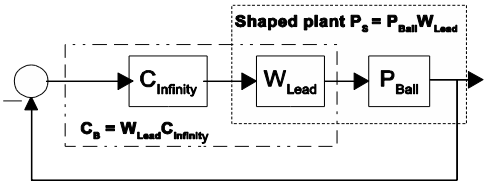

Figure 3. Loop-shaping controller design

In Fig. 3 above, $\mathrm{P_s} = \mathrm{P_{ball}W_{lead}}$ is the shaped plant and $C_\mathrm{B} = W_\mathrm{lead}C_\infty$ is the resultant robust stabilizing controller. The controller denoted as C_∞ was synthesized with `ncfsyn()` Matlab function [12], using a pre-compensator weight $\mathrm{W_{lead}}$ and the transfer function of the ball, $\mathrm{P_{ball}}$ – obtained from the 2nd row of (12) and is given by:

$$P_\mathrm{ball} = \frac{R(s)}{\theta(s)} = \frac{7}{s^2} \tag{23}$$

The weight was selected as follows. The open-loop bode plot of (23) given in Fig. 4 shows that the system has low bandwidth of about $2.5\mathrm{rads}^{-1}$ and the phase is 0 dB (low) at all frequencies. To increase phase, a lead compensator in form of (24) was used to shape the plant.

$$W_{\text{lead}} = k\frac{1+T_{\text{L}}s}{1+\alpha T_{\text{L}}s} \quad (24)$$

where $\frac{1}{\alpha T_{\text{L}}}$ and $\frac{1}{T_{\text{L}}}$ are corner frequencies and k is the gain.

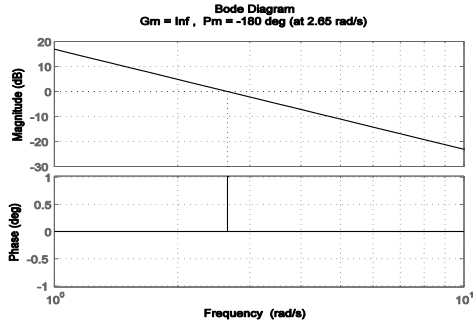

Figure 4. Open-loop response of the rolling ball on beam, P_{ball}

Recall that the required 5% overshoot corresponds to damping ratio of 0.7. The phase margin is related to the damping ratio by the relation [11],

$$\zeta = \frac{P.M.}{100} \quad (25)$$

Thus, a damping ratio of 0.7 requires a phase advance φ of 70^0. The desired settling time for the outer loop is 3.5s so that the inner loop is much faster. A settling time of 3.5s will require bandwidth of between 5 and 6 rads^{-1}, and a center frequency w_{a} of 4 rads^{-1}. The constant α in (24) is given by,

$$\alpha = \frac{1-\sin\varphi}{1+\sin\varphi} = 0.0311 \quad (26)$$

The term $T_{\text{L}} = \frac{1}{w_a\sqrt{\alpha}} = 1.4172$. Substituting T_{L} and α into (24), the resultant weight is,

$$W_{\text{lead}} = k\frac{1.4172s+1}{0.0441s+1} \quad (27)$$

With k = 0.25, the bode plot of the shaped plant $P_{\text{s}} = P_{\text{ball}}W_{\text{lead}}$ shown in Fig. 5 has a bandwidth of 3.2rads^{-1} which means the system will be reasonably fast, there is a phase advance of about 70^0 as desired, and the low-frequency gain is high enough in order to achieve setpoint tracking. Thus, the selected weight in (27) with k = 0.25 was used with the ball transfer function in (23) to synthesize a H-infinity controller C_∞using the `ncfsyn()` matlab function. The robust stabilizing controller $C_{\text{B}} = W_{\text{lead}}C_\infty$ is then applied to the outer-loop as described by the cascade scheme in Fig. 2.

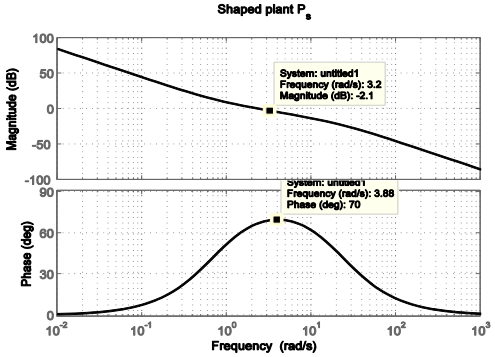

Figure 5. Bode plot of shaped plant P_s when k = 0.25 is the gain of W_{lead}

Fig. 6 also shows that for the loop-shape design, the actual forward loop-shape $L_2 = P_{\text{ball}}C_{\text{B}}$ is very close to the desired shaped plant P_s. The low-frequency gain is high up till about 0.1 rads^{-1} so setpoint tracking and disturbance rejection is expected. The roll-off at the cross over is less than 20 dB per decade for stability, the roll-off rate at high frequencies is about 40dB per decade so noise attenuation is expected and bandwidth is about 3.8rads^{-1} so the system will be reasonably fast. In addition, the robust stability margin $\varepsilon_{\max}$ obtained from the H-infinity synthesis was 0.6 implying that the controller will reject about 60% uncertainties in the coprime factors of the plant for the outer loop. This also means the weight is good enough and the H-infinity controller does not need to do much to meet the required performance.

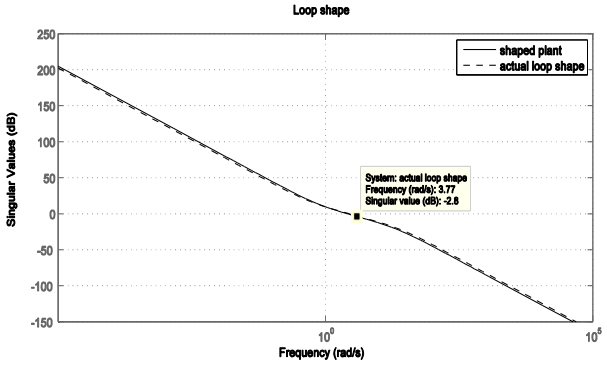

Figure 6. Bode plot of actual loop shape L_1 versus shaped plant P_s

The controller was implemented and simulated in Simulink. The integral gain of the PID controller was slightly adjusted to yield better results. The results are reported next.

V. Results and Discussion

The simulation results show that the H-infinity-PID controller stabilizes the ball on the beam and ensures setpoint tracking on both the nonlinear and linearized BBS. From Fig. 7, the performance is seen to degrade slightly for the nonlinear plant where there is about 7% overshoot. The controller also ensures disturbance rejection in both the linearized and nonlinear BBS when there is a distortion in the ball position due to sharp change in the beam angle.

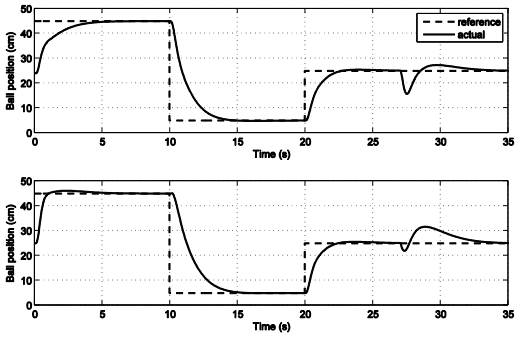

Figure 7. Ball response on linear (top) and nonlinear (bottom) BBS

The settling time is reasonable at 4.5s as seen in Fig. 7 above and the control voltages lie between +12 and -12v even though there is some saturation as shown in Fig. 8. Since most typical

actuators use 12 Volts DC motors, Fig. 8 above means that the proposed control scheme is practicable.

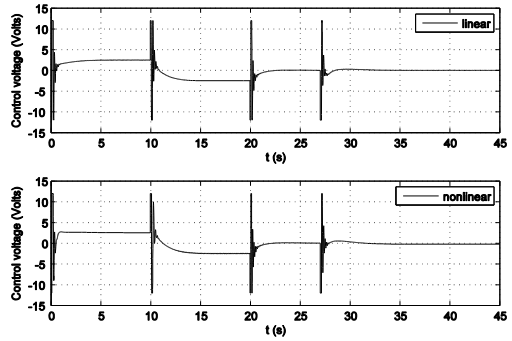

Figure 8. Control inputs for linear (top) and nonlinear (buttom) BBS

In order to analyse the forward loop of the entire cascade scheme depicted in Fig. 2, the closed loop transfer function of the inner-loop of Fig. 2 was computed as $\boldsymbol{T_{\mathrm{M}}} = \frac{\boldsymbol{P_{\mathrm{Motor}} C_{\mathrm{M}}}}{1+\boldsymbol{P_{\mathrm{Motor}} C_{\mathrm{M}}}}$. Thus, the forward-loop for the entire cascade structure is given as $L_2 = P_{\mathrm{ball}} T_{\mathrm{M}} C_{\mathrm{B}}$ and its bode plot is given in Fig. 9.

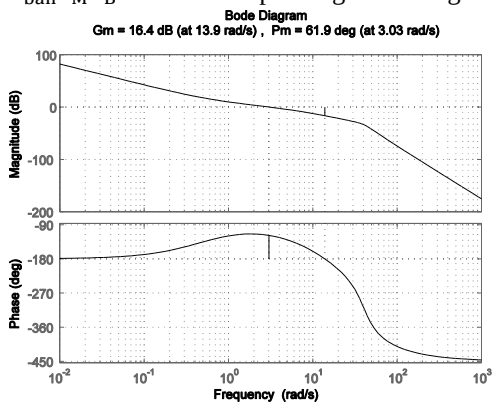

Figure 9. Bode plot of forward-loop of the entire cascade scheme

Fig. 9 shows that the forward-loop of the entire control scheme is able to achieve a phase margin of about 62^0 and a gain margin of about 16.4dB. These high values imply high robustness to uncertainties meaning that the overall cascade control is good.

VI. CONCLUSION

The results of this paper have shown that the proposed H-infinity-PID controller stabilizes the ball on the beam and ensures setpoint tracking, even in the presence of some parametric uncertainties due to neglected terms during modelling. The results have also shown that the proposed controller yielded acceptable performance metrics such as settling time, overshoot and control voltages. The control also yielded high robustness as seen from a robust stability margin of 0.6 from the H-infinity synthesis. However, as per H-infinity methods, such high values signify high robustness at the expense of performance. Again, due to model differences, the controller performance is seen to degrade slightly in the nonlinear plant. And this is expected since the control method proposed in this paper is linear.

REFERENCES

[1] A. Choukchou-Braham, *Analysis and Control of Underactuated Mechanical Systems.* Switzerland: Springer International Publishing, 2014.

[2] K. J. Astrom and R. M. Murray, *Feedback Systems : An Introduction for Scientists and Engineers*. Princeton, N.J.: Princeton University Press, 2008.

[3] T. Kumbasar, "A One to Three Input Mapping IT2-FLC PID Design Strategy," *IEEE Int. Conf. Fuzzy Syst.*, 2013.

[4] J. M. Howe and R. T. O'Brien, "Experimental investigation of optimal PID controller design using model reduction techniques," *Syst. Theory (SSST), 2008 40th Southeast. Symposium*, pp. 31–36, 2008.

[5] D. McFarlane and K. Glover, "A loop-shaping design procedure using H-infinity synthesis," *IEEE Trans. Automat. Contr.*, vol. 37, no. 6, pp. 759–769, 1992.

[6] J. Hauser, S. Sastry, and P. Kokotovic, "Nonlinear Control via Approximate input-output Linearization - The ball and beam Example," *IEEE Trans. Automat. Contr.*, vol. 37, no. 3, pp. 392–398, 1992.

[7] C. G. Bolívar-Vincenty and Beauchamp-Báez, "Modelling the Ball-and-Beam System From Newtonian Mechanics and from Lagrange Methods," *Twelfth LACCEI Lat. Am. Caribb. Conf. Eng. Technol.*, vol. 1, pp. 1–9, 2014.

[8] P. E. S. Wellstead, *Introduction to physical system modelling*. London: Academic Press, 1979.

[9] D. N. Abara, "Modelling, Simulation and Control of the Ball and Beam System," M.Sc. dissertation, School of Elect. & Elect. Eng., Univ. of Manchester, England, 2015.

[10] P. J. Antsaklis, *A Linear Systems Primer*. Boston, MA: Birkhauser Boston, 2007.

[11] K. Ogata, *Modern Control Engineering*, 5th ed. Boston ; London: Pearson, 2010.

[12] K. Glover and D. McFarlane, "Robust Stabilization of Normalized Coprime Factor Plant Descriptions with H-infinity-bounded Uncertainty," *IEEE Trans. Automat. Contr.*, vol. 34, no. 8, pp. 821–830, 1989.